Arch. Metall. Mater. **65** (2020), 1, 27-37

DOI: 10.24425/amm.2019.131093

M. BARTOSIEWICZ[1*], A. CWUDZIŃSKI[1]

INFLUENCE OF MODERN LADLE SHROUD ON HYDRODYNAMIC STRUCTURE IN ONE STRAND SLAB TUNDISH

In the presented work, the numerical simulations results of the liquid steel flow in the one strand tundish were shown. Influence of the modification and immersion depth in the liquid steel of the ladle shroud and subflux turbulence controller on hydrodynamic structure of the liquid steel movement in the working space of tundish were examined. The ladle shroud shape modification consisted on the decompression and compression of the main supplying stream of the tundish. The mathematical model used in the numerical simulations through physical modeling and industrial trials were validated. The numerical simulation results (using four variants of the modified ladle shroud immersion depth in the liquid steel) in the isothermal conditions using laboratory experiments on the water model were verified. Whereas, the numerical simulation results (using one of the tundish research variant) for non-isothermal were compared with the results from the industrial measurements. Three turbulence models: Realizable k-ε, RNG k-ε and SST k-ω were used in the computer calculations (performed via the Ansys-Fluent computer program). In order to obtain the actual view of the liquid steel flow hydrodynamic structure in the examined tundish for the two mathematical models using different turbulence models, which were most similar to the laboratory experiments and industrial measurements, the numerical simulations were performed in the non-isothermal conditions. The application in the computer calculations of the SST k-ω turbulence model caused the smallest differences between the numerical simulations, laboratory experiments and industrial measurements. Performed tests showed that ladle shroud can be used as a flow control device and the modified ladle shroud immersion at a depth of 0.1 m in the liquid steel caused the shortest range of the transition zone among the tested cases.

Keywords: continuous steel casting, tundish, ladle shroud, liquid steel flow, turbulence models

Nomenclature

k Turbulent kinetic energy (m^2s^{-2}),
u Liquid steel flow velocity (ms^{-1}),
ε Dissipation rate of kinetic energy (m^2s^{-3}),
d Ladle shroud diameter (m),
ω Specific dissipation rate of the turbulent energy ($1s^{-1}$),
C_μ Model constant (-),
F Dimensionless concentration of the tracer (-),
C_t Concentration of the tracer in time (wt%),
C_0 Initial concentration of the tracer (wt%),
C_∞ Final concentration of the tracer (wt%),
Θ Dimensionless time (-),
t Residence time (s),
V Volume of liquid steel in the tundish (m^3),
$\dot{v}$ Volume flow rate of the liquid steel (m^3s^{-1}),
D_{Fcurve} Percentage average difference between average measurement point location and F curve from the numerical simulation (%),
ΔC_t Dimensionless tracer concentration difference in t time between the potassium chloride KCl concentration from the water modeling (or the recorded element concentration from the industrial trials) and the tracer concentration from the numerical simulation (-),
N_M Number of the measurements for each laboratory experiments/industrial trials (-).

1. Introduction

The continuous steel casting method in the industry has been used for decades. At this time, continuous casting of steel has become the leading process used for the production of the semi-finished steel product. The idea of this process is continuous influent of the liquid steel to the casting mold or few casting molds, for which the tundish is responsible. Therefore, the improvement of the tundish working conditions is a significant aspect from the point of view the optimization the operation of

[1] CZĘSTOCHOWA UNIVERSITY OF TECHNOLOGY, FACULTY OF PRODUCTION ENGINEERING AND MATERIALS TECHNOLOGY, DEPARTMENT OF METALLURGY AND METALS TECHNOLOGY, 19 ARMII KRAJOWEJ AVE, 42-200 CZĘSTOCHOWA, POLAND

* Corresponding author: bartosiewicz.michal@wip.pcz.pl

the whole CSC process. The improvement of the liquid steel flow hydrodynamic structure in the tundish is associated with an increase active flow (plug and ideal mixing flow). The right ratio of the plug and ideal mixing flow, the range of the transition zone can be shortened, while mixing various steel grades during the sequential casting process [1-3]. This effect can be obtained through interfering with the tundish working conditions. One of the main ways to optimize and improve the hydrodynamic conditions of liquid steel flow in the tundish is the adaptation of the flow control devices FCD in the tundish working volume [4-8]. Performing research in the industrial conditions is characterized by difficulties due to high research costs and continuity of the production process. Therefore, the numerical and physical simulations (performed on water models) have been widely used. In the work [9], the influence of subflux turbulence controller STC installation and its construction on the transition zone and the shape of the percentage volume of the liquid steel flow in a two strand T type tundish were investigated. The application of the FCD caused the reduction of the transition zone, whereas the percentage of the active liquid steel flow increased in relation to the results obtained using tundish without interfering in its working volume. The installation of the FCD in the tundish is selected by the individual, due to the shape and number of outlets in the tundish. That requires research works directed on the specific type of the tundish. A new research trend is to use the ladle shroud as a FCD, which the primary task is to protect the feeding metal stream from the steel ladle to the tundish against secondary oxidation. The interference on the ladle shroud shape influences on forming the tundish main supplying stream, which in a result influences on liquid steel flow hydrodynamic structure in the tundish. A number of the research results related to the ladle shroud modification are known, which were mentioned in [10]. Each of the ladle shroud proposals is characterized by a significant advantages and disadvantages. However, a group of ladle shrouds [11-13], which modification consists on the compression and decompression (SLS – Swirling Ladle Shroud, DLS – Dissipative Ladle Shroud) or only decompression (TLS – Trumpet Ladle Shroud) of the main supplying stream, it has characterized the special advantage, which is versatile of the use in the different types of the tundish (regardless of its shape and number of outlets). This provokes the possibility of the integration the modified ladle shroud with the other FCD, which may bring a significant benefit due to the tundish's operating conditions. In the work [13], the influence of the ladle shroud working space modification (TLS) on liquid steel flow hydrodynamic structure in the one strand tundish was examined. The decompression of the main supplying stream a decrease of the liquid steel flow velocity in the ladle shroud volume was caused. An analysis of the flow volumes was performed, which showed an increase of the volume of the active liquid steel flow using TLS in relation to the results obtained using the conventional ladle shroud CLS.

This paper presents the results of the numerical and physical simulations of the liquid steel flow in the tundish using the modified ladle shroud MLS. Furthermore, the mathematical models used in calculations was verified by industrial experiments (during industrial experiments used tundish equipped with subflux turbulence controller and conventional ladle shroud). Also, the integration of MLS and STC was checked. Likewise, liquid steel flow in the tundish without the subflux turbulence controller and with CLS was examined. The effect of the change the MLS immersion depth in liquid steel on the hydrodynamic structure in the tundish was checked.

2. Examined object characteristic and research methodology

The research object is the one strand tundish designated to the continuous casting of slabs. The tundish nominal capacity of 30 Mg is characterized. The working volume of the object expands towards to the tundish outlet zone, therefore it is the wedge-type tundish. The tested object is equipped with a dam with two overflow windows, which is installed before the place of the lowering the tundish bottom. The primary purpose of that device is to reduce the flow velocity of the liquid steel wave at the beginning of the casting sequence. The control of the liquid steel flow from the tundish to the casting mold is carried out using a stopper rod system. Detailed information of the tested tundish is described in detail in [14,15]. The essence of the research is to equip the discussed tundish in MLS, through which liquid steel flows into the tundish from the steel ladle. This modification consists on interfering in the construction of the ladle shroud at its final section, by changing its diameter. The modified part of the ladle shroud consists with three elements. The first element decompresses, the second compresses and the third decompresses again the main supplying stream of the tundish. Five ladle shroud immersion depths in the liquid steel were checked (table 1 shows specific information's about the research cases). The numerical simulation results of the cases 1-4 on the tundish physical model were verified. Physical simulator is made of glass, on a 2:5 scale and has characterized by a nominal capacity of 210 L. The modified section of the ladle shroud was made using stereolithography method. The liquid flow in the physical model is controlled through the hydraulic system and the flow meter. On the figure 1a the tundish inlet zone of physical model and the virtual model of the discussed tundish with MLS immersed to a depth of 0.1 m in liquid steel is showed. Figure 1b presents the dimensions of MLS. However, in order to obtain more fully verification of the mathematical model used in calculations, industrial measurements on the continuous steel casting machine were carried out in the one of the Polish Steelworks (case 8). During industrial experiments, the tundish was equipped with a subflux turbulence controller, which was tested in work [16]. Figure 1c presents the tundish virtual model equipped with a STC and CLS (case 8) and shows the tundish inlet zone of the case 6 and 7.

In this work, the research cycle consisted of three stages. The first concerned the performance of the virtual tundish objects and numerical simulations of the liquid steel flow in the tundish for isothermal conditions. The second was related to the

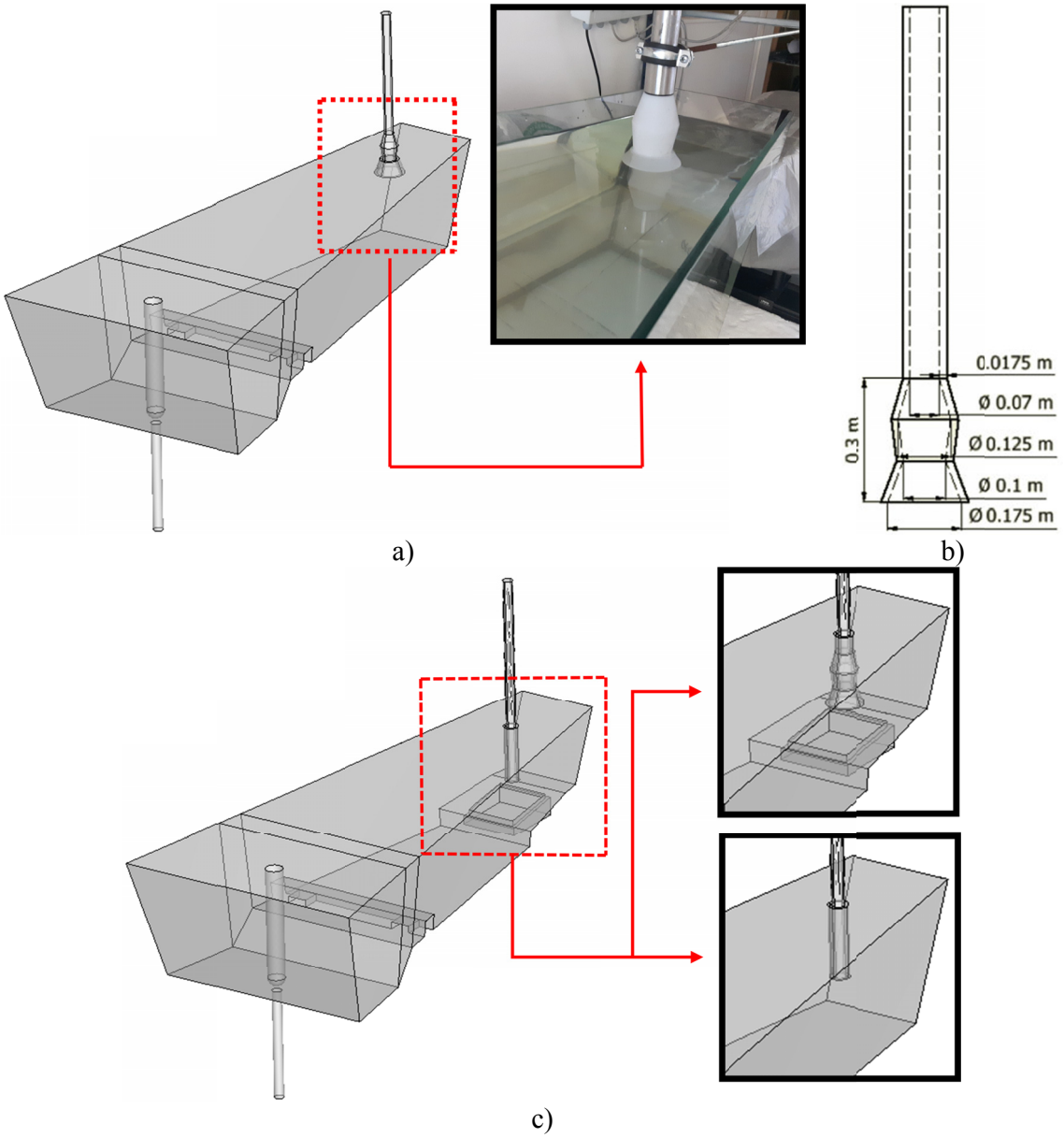

Fig. 1. The considered research cases: a) case 1 with inlet zone of the tundish physical model with MLS immersed in the water, b) dimensions of the MLS, c) industrial tundish and tundish inlet zone of the cases 6 and 7

TABLE 1

The juxtaposition of the considered research cases

Case no.	Ladle shroud type	Tundish equipped with a STC	Ladle Shroud immersion depth in liquid steel [m]
1	MLS	×	0.10
2	MLS	×	0.15
3	MLS	×	0.20
4	MLS	×	0.25
5	MLS	×	0.40
6	MLS	✓	0.40
7	CLS	×	0.40
8	CLS	✓	0.40

verification of the mathematical model used in the calculations, by the use of the physical model research (for the cases 1-4) and the industrial measurements (the verification the numerical simulation results in the non-isothermal conditions – the case 8). The third stage of the research concerned the performance of the numerical simulations in the non-isothermal conditions using the most favorable turbulence model.

The virtual models of the tudnish in the Gambit computer program were made. In order to create 3D objects reflecting the tested tundishes the "bottom-up" and Boolean method were used. Then, the virtual objects were discretized using a computational grid, which consisted from 218000 to 330000 of the control volumes depending on the considered research cases. The tundish virtual models were exported to the Ansys-Fluent computer program, which was used to perform the numerical simulations of liquid steel flow in the discussed tundish. The phenomena of the shape the liquid steel flow hydrodynamic structure in the tundish and the ladle shroud working volume were calculated using a mathematical model, described in detail

in [14]. Three mathematical models with different the turbulence model: Realizable k-ε, RNG k-ε and SST k-ω in the computer calculations in the isothermal conditions were tested, which were more characterized in the works [11,17,18]. The numerical simulations of the cases 1-4 were repeated using one of the three mentioned turbulence models. The results of computer calculations were verified by the performance of the laboratory tests on the physical model of the tundish. This allowed to the selection of the optimal turbulence model in the numerical simulations of the liquid steel flow in the tundish for the non-isothermal conditions. The results of the research presented in work [14] indicate that the use in the calculations the Realizable k-ε turbulence model, correlated with the results from the experiments performed on the water model. However, taking into account the ladle shroud in the tested object, through the simulation of liquid steel flow in the ladle shroud entire space (from steel ladle to tundish), can affect on the distribution of the liquid steel streams and the formation of the turbulence in the considered tundish. Therefore, the mathematical model was re-verified using the RNG k-ε turbulence model and the calculations were enriched using the SST k-ω turbulence model. The complement the verification of the mathematical model used in the computer calculations using the three mentioned turbulence models was the comparison of the numerical simulation results in the non-isothermal conditions with the outcomes from the industrial trials (for the tundish case 8). The studies were carried out by simulating the continuous casting process of a slab characterized by the dimensions of 1.5 × 0.225 m (with a casting velocity of 0.015 ms^{-1}). The upper surface of the tundish model was characterized by zero tangential stresses, and was imitated the boundary between liquid steel/tundish powder. The heat losses from the examined object were taken into account in the computer calculations in the non-isothermal conditions, which are described in detail in the work [14]. The mathematical model included the entire space of the ladle shroud from its connection to the steel ladle. This allowed to the simulation of the metal movement in the ladle shroud volume (especially significant in the tundish cases equipped with the MLS). In the boundary condition corresponding to the place of flowed liquid steel to the ladle shroud, the following parameters were used: velocity of the liquid steel flow 1.316 ms^{-1}, temperature of the liquid steel 1813 K, turbulent kinetic energy 0.0173 m^2s^{-2}, turbulent dissipation rate of kinetic energy 0.06514 $m^{-2}s^{-3}$ (for variants using the Realizable k-ε and RNG k-ε turbulence models), specific dissipation rate of turbulent energy 4.410714 $1s^{-1}$ (for variants using the SST k-ω turbulence model). The values of the turbulent kinetic energy, the turbulent dissipation rate and the specific dissipation rate were counted using the following equations [11,17,19]:

$$k = 0.01u^2 \tag{1}$$

$$\varepsilon = \frac{2k^{1.5}}{d} \tag{2}$$

$$\omega = C_\mu^{0.75}\frac{k^{0.5}}{0.07d} \tag{3}$$

The physicochemical properties of the liquid steel were adopted in the simulations: viscocity 0.007 $kgm^{-1}s^{-1}$, thermal conductivity 41 $Wm^{-1}K^{-1}$, heat capacity 750 $Jkg^{-1}K^{-1}$. The density of the liquid steel was constant (7010 kgm^{-3}) in the computer calculations in the isothermal conditions, whereas in the numerical simulations in the non-isothermal conditions, the density of the liquid steel was calculated from a polynomial of the temperature, which are described in the work [14]. The mathematical model, which describe the liquid steel flow in the tundish was solved using the method of control elements integration through the second order discretization method. In order to describe the coupling of pressure and velocity fields, Semi-Implicit Method of Pressure-Linked Equations-Consistent SIMPLEC was used. The User Defined Scalar UDS transport equation to solve the tracer flow in the working volume of the considered model was applied. The results of the numerical simulation of the liquid steel flow in the isothermal conditions (cases 1-4) was the determination of an F-type RTD (Residence Time Distribution) curve, i.e. a graphical characterization of the mixing moment in the tundish of the two casted successively steel grades (transition zone). The generation of the F curve consists in entering the tracer into the ladle shroud (continuous signal) and recording its concentration at the exit of the tested object. The units of concentration and time in the F-type RTD curve converted into dimensionless values using the following equations [15,20,21]:

$$F = \frac{C_t - C_0}{C_\infty - C_0} \tag{4}$$

$$\Theta = \frac{\tau}{V\dot{v}^{-1}} \tag{5}$$

The determination of the F curve in the isothermal conditions allowed to verify the mathematical model and type of the turbulence model used in the computer calculations through performing tests on a physical model. The liquid medium that simulated liquid steel during laboratory measurements was water, due to the similar kinematic viscosity at 20°C, as liquid steel at 1600°C. During the performed measurements on the water model, the Froude criterion was taken into account. Therefore, the criterion of the similarity of the gravitational and the inertial forces between the tundish in the industrial conditions and the water model was provided [5,22,23]. The generation of the F curve during the performed research on the water model consisted on recording the change in the salinity concentration of the water, which flow through the simulator. A water simulating another cast steel grade was supplied to the MLS and the tundish through a hydraulic system. The mixing moment of the two steel grades in the tundish was simulated through introducing a tracer (potassium chloride KCl) to the water model. The change in the salinity concentration was recorded using a conductometric sensor, which in the outlet of the tundish was installed. The water salinity measurement was recorded every 10 s through 2 dimensionless time. Each laboratory experiments were repeated six times for each research case. The obtained

measure points (after conversion into the dimensionless values) were compared with the curves *F* obtained from the numerical simulations in the isothermal conditions, which allowed for the analysis of the points and curves distribution.

The verification analysis was divided into the two stages. First, the visually judgment was performed, which consisted on the assessment the differences between the individual curves and the measurement points (the quality analysis). Next, the percentage average differences between average measurement point location and the *F* curve from the numerical simulations were calculated by the use of the equation 6 (the quantity analysis).

$$D_{Fcurve} = \frac{\sum_{\Theta=0}^{2} \Delta C_t}{N_M} \times 100\% \quad (6)$$

Then, using the case 8 the numerical simulations of the liquid steel flow (repeating three times the calculations using one of the mentioned turbulence model) in the non-isothermal conditions was performed. Thanks to that, the *F* curves were generated, which allowed to verify the simulation results by the industrial measurements. The generation of the *F* curve in the industrial conditions consisted in the examination the chemical composition of the liquid steel during the mixing of the two liquid steel grades in the tundish (during the transition from one cast steel grade to another, while the sequential casting process). It was done by taking samples of the liquid steel from the casting mold. First samples was taken during opening the steel ladle with a second cast steel grade. A total of 14 samples of the liquid steel from the casting mold during the transition zone were taken. The entire operation was repeated four times for the four different transition zones. After the measurements, the steel samples were subjected to the spectral analysis. Due to a change in the chemical compositions between the individual samples, it was able to generate the measurement points (after conversion into the dimensionless values), which was compared with the *F* curve from the numerical simulations. The verification analysis using a method like previously mentioned (in the water modeling analysis) was performed. Whereas, the industrial experiments for 3 dimensionless times were lasted.

The use of the selected turbulence model during the verification of the mathematical model, the numerical simulations in the non-isothermal conditions of the liquid steel flow hydrodynamic structure in the all considered research cases were performed. Particular attention was paid to the directions of the liquid steel flow in the tundish working space. Furthermore, the analysis of the transition zone during sequential casting process was performed. According to a literature review, the transition zone was being modified depending on the cast steel grade and the type of slab [24,25]. In this work, the transition zone in the range from 0.2 to 0.8 of the dimensionless concentration is determined. This range is dedicated to the continuous casting of slabs, using the analyzed tundish, as described in the works [15,26].

3. Results of examination

3.1. Laboratory experiments and isothermal numerical simulations

The result of the numerical simulations in the isothermal conditions and the physical research on the water model was the generation of the RTD type *F* curves. Figure 2 shows the results of the numerical and physical simulations. In the case with immersed MLS on a depth of 0.1 m in the liquid steel, the implementation of the Realizable *k-ε* turbulence model resulted a faster achievement of the dimensionless concentration (next cast steel grade) in the relation to the simulations using the SST *k-ω* and RNG *k-ε* turbulence models in the range from 0.2 to 0.8 of the dimensionless time. After reaching 0.5 of the dimensionless concentration, the shape of the individual *F* curve were slightly different. In the case 2 (Fig. 2b), the *F* curves from the simulation using the Realizable *k-ε* model faster reach the dimensionless concentration in the relation to the results of the calculations using the RNG *k-ε* and SST *k-ω* turbulence model (in the range from 0.18 to 1 of the dimensionless time). Whereas, after reaching 0.65 of the dimensionless concentration, this trend is reversed. In the case 3, slight differences in the shape of the *F* curves from simulations using the SST *k-ω* and RNG *k-ε* were observed. The use of the Realizable *k-ε* model caused a faster the obtainment of a dimensionless concentration in the range from 0.1 to 1 of the dimensionless time in relation with the other results of the numerical simulations. In the case 4 (Fig. 2d) in the range from 0.2 to 1 of the dimensionless time the *F* curve from the simulation using the SST *k-ω* model faster obtaining the dimensionless concentration compared to the simulation result including the Realizable *k-ε*. After recording the dimensionless concentration on 1 level, the shape of *F* curves were slightly different (for numerical simulations using Realizable *k-ε* and SST *k-ω* turbulence models). *F* curve, which was being generated on the basis of the numerical simulation results using the RNG *k-ε* model, the dimensionless concentration was being reached a bit slower than to the other simulation variants (in the MLS immersed on 0.25 m variant) in the range up to 1.4 of the dimensionless time. The differences in the outcomes of the simulations resulting from the type of turbulence model proves the right of using the verification of mathematical model used in the calculations. The distribution of the measurements points from experiments on a water model was compared with the results from numerical simulations in the isothermal conditions. The use in the calculations the SST *k-ω* and Realizable *k-ε* turbulence model, the smallest discrepancies in the position of the *F* curve were observed with the measurements points obtained from laboratory experiments in comparison to the other numerical simulation results in the tested cases 1-4.

Figure 3 presents the results of the quantity analysis. The presented graph shows the percentage average difference between the average measurement point location (the water model) and the F curves from the numerical simulations (for the cases 1-4). It can be seen that the lowest differences are visible

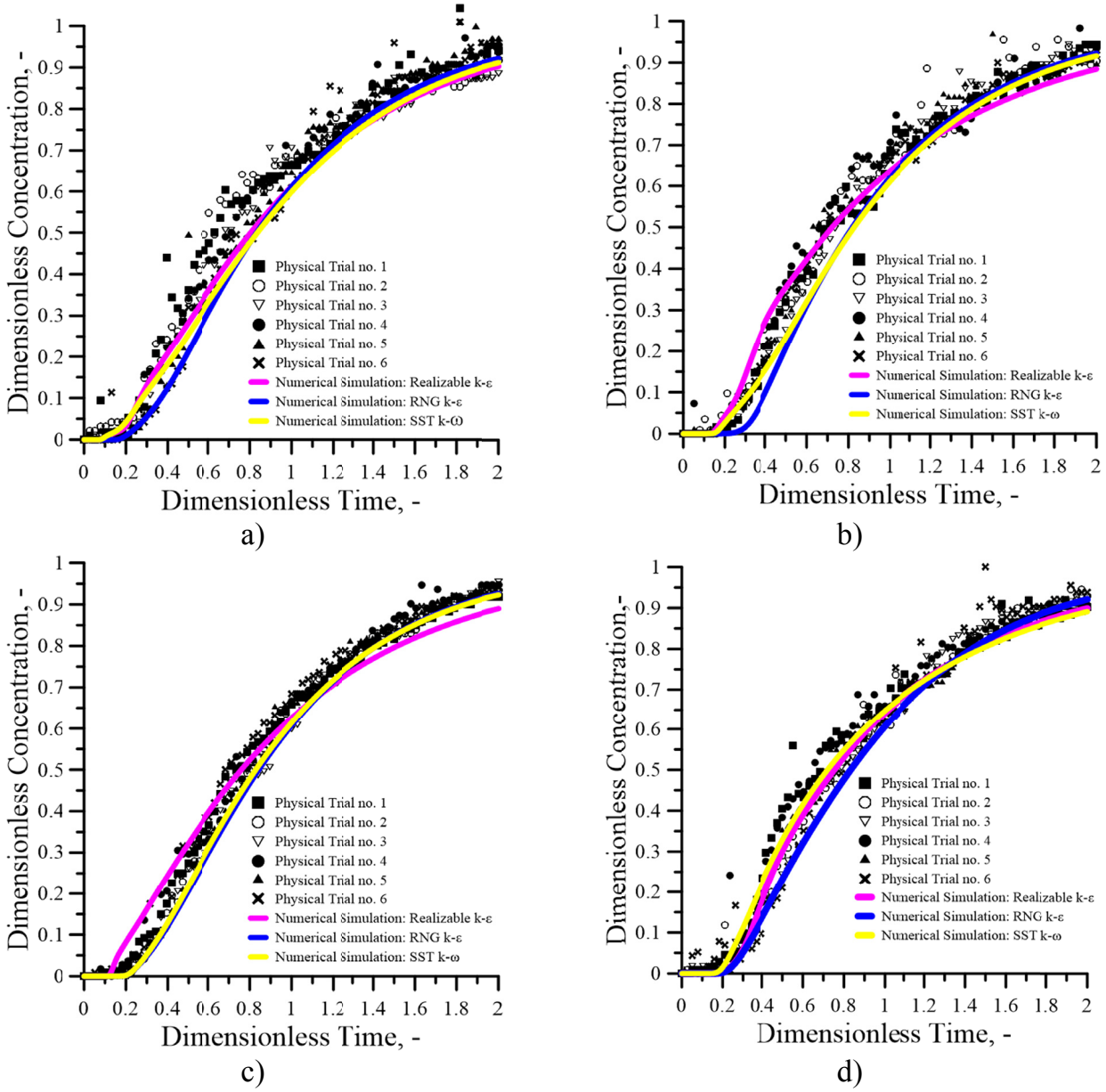

Fig. 2. The *F* curves for the numerical simulations in the isothermal conditions in the relation with the physical trials: (a) case 1, (b) case 2, (c) case 3, (d) case 4

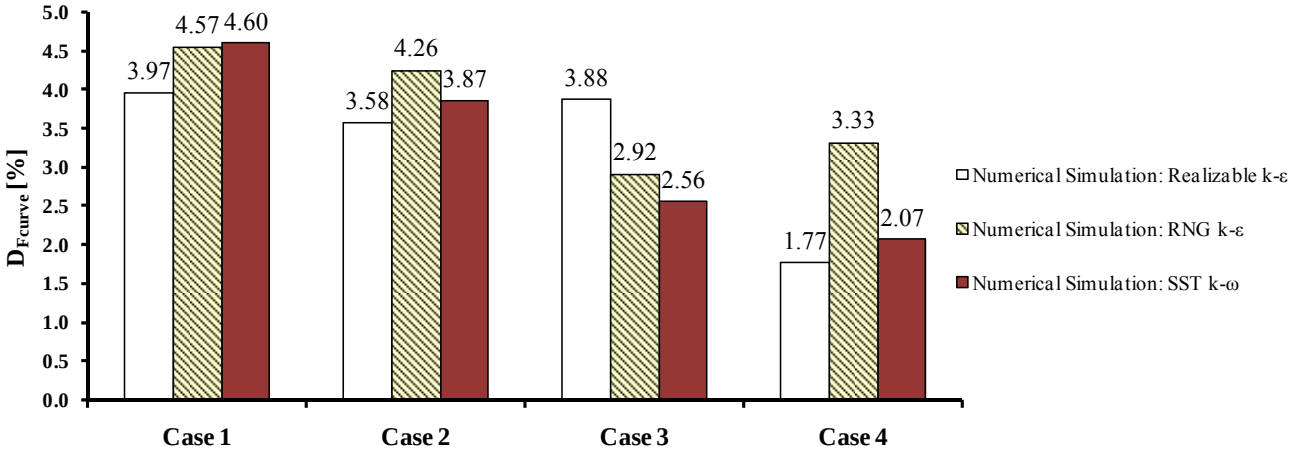

Fig. 3. The percentage average differences between the average measurement point location (the water model) and the *F* curve from the numerical calculations

by the use the Realizable *k-ε* turbulence model in the numerical calculations (only results of the case 3 are an exception). Besides, the best correlation between the physical experiments and the mathematical calculations in the case 4 was reached (1.77%). In general, the use of the RNG *k-ε* turbulence model caused the biggest divergences among the tested turbulence models. Whereas, the results of the numerical simulations using the SST *k-ω* turbulence model indicated the similar values to the outcomes obtained by the use the Realizable *k-ε* in the cases 2 and 4 (about 0.3%). Nevertheless, in the case 3 the mentioned turbulence model brought the best correlation with the real turbulence nature (the difference was equal 2.56%).

3.2. Industrial trials

The verification of the mathematical model used in the computer calculations was supplemented by a comparison of the computer calculation results in the non-isothermal conditions with outcomes from the industrial measurements, considering the three turbulence models (Realizable *k-ε*, RNG *k-ε*, SST *k-ω*). The verification of the mathematical model on the tundish case 8 was carried out. During the industrial measurements, the transition zone was tested, while the sequential casting process. The distribution of the industrial measurement points with the results from the numerical simulations was compared (Fig. 4). The analysis of the *F* curves showed that in the range from 0.3 to 1.25 of the dimensionless time, the *F* curve from the numerical simulation using the Realizable *k-ε* turbulence model slowly reaches the dimensionless concentration in relation to the results from numerical simulations using the RNG *k-ε* and SST *k-ω* turbulence model. In the other locations of the *F* curves, the slight differences between each other were noted. Besides, in general, all of the tested turbulence models were characterized by a well convergences with the industrial trials. Only in the variant with the Realizable *k-ε* turbulence model, the slight divergences from 0.3 to 1.25 of the dimensionless time were visible.

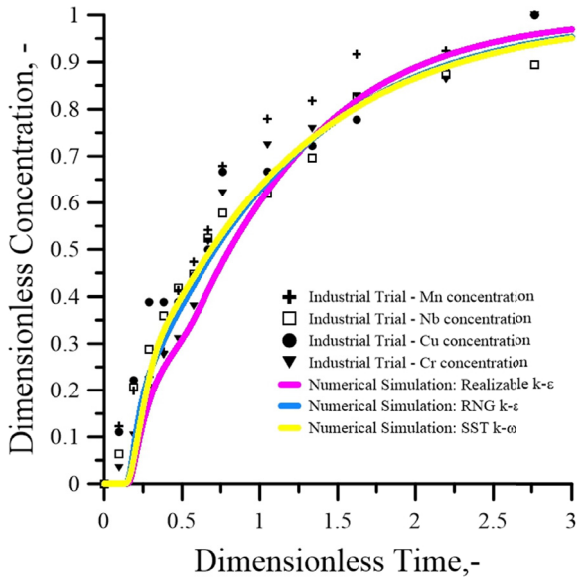

Fig. 4. The *F* curves for numerical simulations in the non-isothermal conditions in relation with industrial measurements (case 8)

In order to confirm the mentioned conclusions, the quantity analysis was performed. The percentage average differences between the average measurement point location and the *F* curves from the numerical simulations using the Realizable *k-ε*, RNG *k-ε* and SST *k-ω* turbulence model were calculated and D_{Fcurve} presents as follows: 7.12% (Realizable *k-ε*), 4.10% (RNG *k-ε*), and 3.83 (SST *k-ω*).

3.3. Summary of verification research

The performed verification studies in this chapter were summarized. Figure 5 presents level of the correlation numerical simulation results with the water modeling and industrial trials results. The graph based on received D_{Fcurve} from quantity analysis (water modeling and industrial trials), for each cases under verification was performed. Ranks have been assigned to the individual turbulence models, where level 1 means the best correlation, whereas level 3 the worst convergence numerical simulation results with the actual outcomes. The received ranks, for the individual cases were pointed out, which then were connected by a lines. The areas for the generated geometries (limited by lines and XY axis) for each turbulence model ranks were calculated (distance between individual labels on XY axis were equal 1). The indication of the turbulence model, which rank strives to 1 was the objective of the mentioned analysis (the lowest area of the generated geometry the better correlation of the indicated turbulence model with the actual hydrodynamic structure).

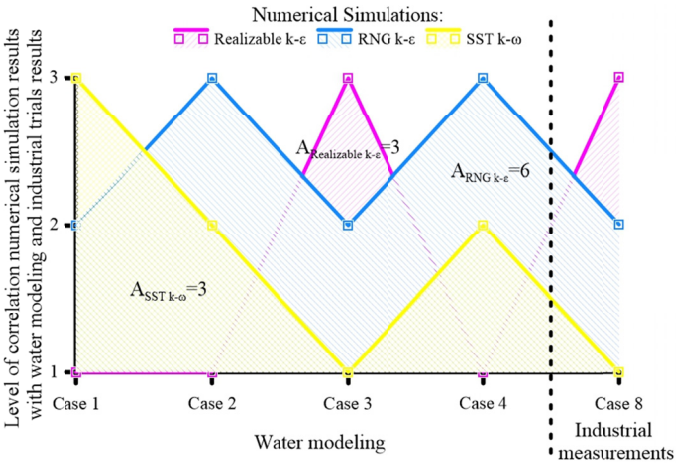

Fig. 5. The analysis of the correlation numerical simulations results with water modeling and industrial trials results

It can be seen that the water modeling verification indicates the Realizable *k-ε* turbulence model as the best correlating with the actual turbulence flow. Only in the case 3, the Realizable *k-ε* received third rank. Whereas, based on the industrial measurement outcomes, the SST *k-ω* turbulence model the highest

convergences were turned out. Therefore, in general, the use of the Realizable k-ε or SST k-ω turbulence model is more accurate than the use of the RNG k-ε in the considered research variants. Besides, it can be put forward the similar conclusions by taking into account the calculated areas (areas of the generated geometries for the Realizable k-ε and SST k-ω were equal 3). Therefore, the Realizable k-ε and SST k-ω turbulence models in the non-isothermal numerical simulations were taken into account.

3.4. Non-isothermal numerical simulations

The figure 6 shows the liquid steel flow fields in the space of the considered tundish variants using the Realizable k-ε turbulence model in the calculations. On the plane being the symmetry of the considered research object, the results were presented. For easier analysis of the distribution of the flow fields, the tundish was divided into three research zones: the inlet zone (influence zone of the main supplying stream), the outlet zone (zone with lowering the tundish bottom behind the dam) and the central zone (located between the inlet and outlet zone). The analysis of the liquid steel flow fields shows that the use of MLS and changing its position influences on the hydrodynamic structure in the examined tundish. In the inlet zone, a circulating stream in the cases 2, 3, 4 and 5 between the right sidewall and bottom of the tundish was observed. In case 1, from the inlet zone to central zone of tundish, a wide influence of the horizontal circulation stream, which acts from the tundish bottom to the upper surface of the object was noticed. In the tundish central zone, a circulating stream in cases 2, 3, 4 and 5 near tundish bottom was observed (between mentioned variants a slightly differences in its position and shape were noted). Furthermore, in case 5 the horizontal circulation stream above the right edge of the dam was observed. Analyzing the cases 6 and 8, it was noted that the use of STC suppresses the momentum of the main supplying stream and directs it towards the liquid steel/tundish powder boundary. However, the biggest difference between the cases 6 and 8 in the central zone of the tundish were noticed, where in the case 8 a wide influence of the horizontal circulation stream was generated. In the case 7, the lack of modification in the tundish inlet zone generates a circulation stream between the right sidewall and the bottom of the tundish (in the tundish inlet zone). Whereas, in the tundish central zone a circulating stream near the tundish bottom was observed. Furthermore, in the tundish outlet zone, the influence of the backflows in the all research cases were noticed.

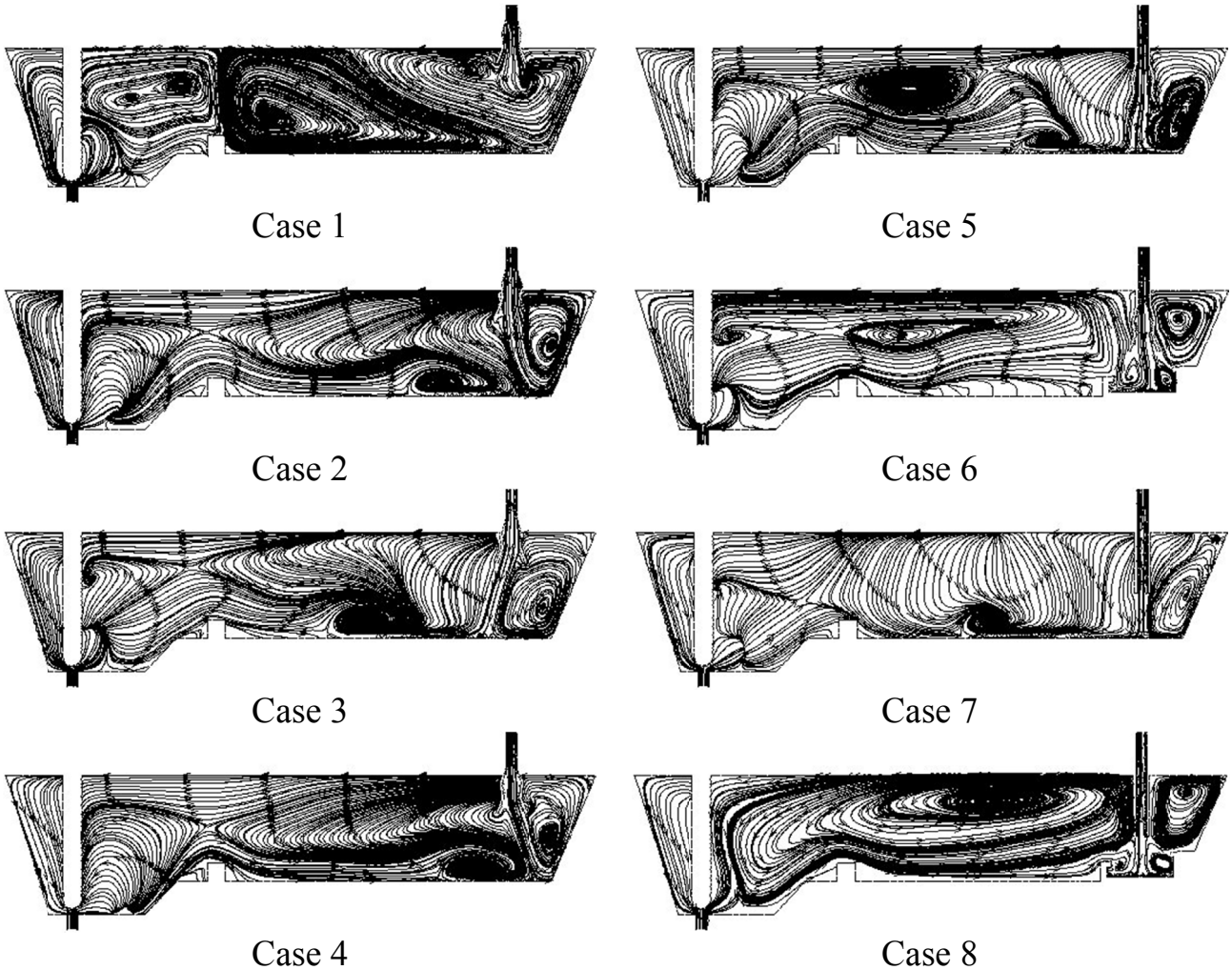

Fig. 6. The fields of the liquid steel using the Realizable k-ε turbulence model in the numerical simulations in the non-isothermal conditions

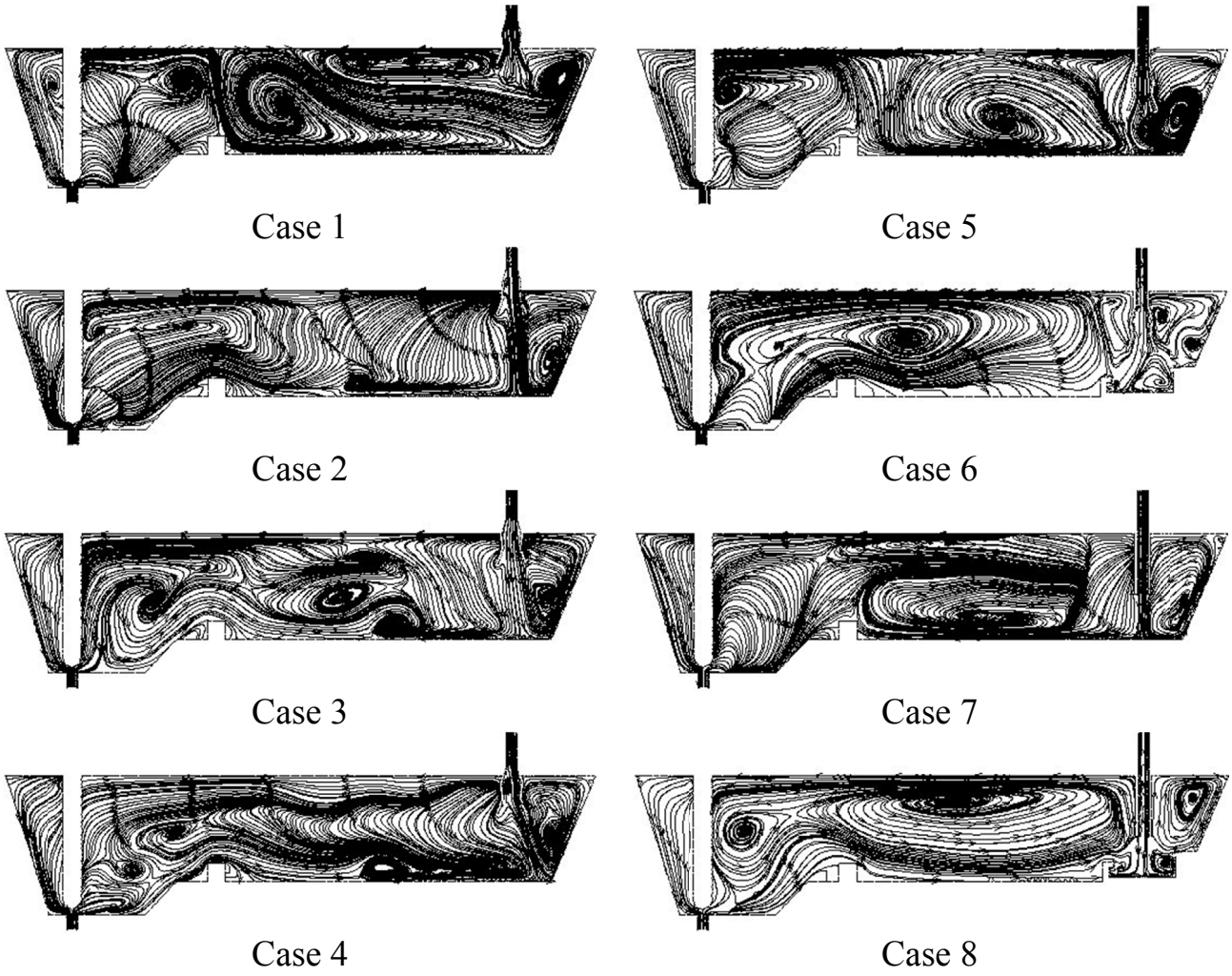

Fig. 7. The fields of the liquid steel using the SST *k-ω* turbulence model in the numerical simulations in the non-isothermal conditions

Then, the analysis of the liquid steel flow fields using the SST *k-ω* turbulence model in the computer calculations were performed (Fig. 7). Generally, the analysis showed that the use of the SST *k-ω* turbulence model compared to the results using the Realizable *k-ε* turbulence model causes the increase of the number of the circulation streams in the tundish working space and the changes their shape and position. The largest differences in the tundish case 1, 3, 5 and 7 were observed. In the case 1, the influence of the horizontal circulation stream along the liquid steel/tundish powder boundary in the tundish central zone was noticed (also a wide influence of a circulating stream from the bottom and the upper surface of the tundish was observed). Likewise, in the tundish inlet zone the vertical circulation stream between a right sidewall and upper surface of the tundsish was noticed. In case 3, the use of the SST *k-ω* turbulence model resulted in enriching the central and outlet tundish zone with the circulation streams. Whereas, in the cases 5 and 7 a wide influence of the horizontal circulation stream was noticed.

The next stage of the research was to check the transition zone during the sequential casting process. The obtained results allowed to calculate a mass of transition slab using individual examined cases. Figure 8 presents masses of the transition slab using all research cases (results from the numerical simulations in the non-isothermal conditions) with relation between outcomes using the Realizable *k-ε* and the SST *k-ω* turbulence model. The consideration of the transition slabs using in the numerical calculations the SST *k-ω* model shows that the use of the MLS in all tested variants of its immersion depth in the liquid steel shortens the range of the transition zone in relation to the industrial results (case 8). The shortest range of the transition zone for case 1 (25.95 Mg) was achieved. Furthermore, the coupling of STC and MLS causes widening the transition zone (33.69 Mg) in relation to the other cases. Whereas, in the case without modification of the tundish inlet zone (case 7) was cast 31.30 Mg of transition slab. In general, the use of the Realizable *k-ε* turbulence model in the computer calculations the similar tendency of the formation the transition zone in relation to the outcomes using SST *k-ω* turbulence model was caused. Also, the use of MLS shortens the range of transition zone in relation to the industrial outcomes (only in the cases 3 and 6 the transition zone were longer). Nevertheless, the most favorable case in terms of the transition zone formation was variant with MLS immersion depth in the liquid steel at 0.1 m) for both turbulence models.

An analysis of the turbulence intensity at the end of the ladle shroud, considering the most favorable variant (case 1) and the case from industrial conditions (case 8) was performed. The turbulence intensity through the ratio of the turbulent kinetic energy and the liquid steel flow velocity is described [16]. The initial turbulence intensity on the ladle shroud inlet in the considered cases was calculated at 0.1. The turbulence intensity on the end diameter (on the line) of the ladle shroud (in cases 1 and 8) was recorded (Fig. 9). In the case 1, the highest turbulence intensity values in the 0.02 m position of ladle shroud diameter was achieved (for the Realizable *k-ε* and SST *k-ω* turbulence model was equaled 0.14 and 0.12, respectively). Whereas, the lowest turbulence intensity values in the – 0.0875 m position of the ladle shroud diameter were observed (near the ladle shroud wall). Furthermore, the use SST *k-ω* turbulence model in the calculations the lower turbulence intensity values on the ladle shroud end was caused. However, in the case 8 that tendency was reversed. The highest turbulence intensity values near ladle shroud refractory was recorded, whereas the lowest in the middle of main supplying stream. Therefore, it can be noted that the use of MLS results in less erosion of the ladle shroud refractory at its end compared to the use a conventional ladle shroud.

4. Summary

The implementation of the innovative technology in the industrial conditions is burdened with earlier simulation tests. The results of the computer simulations are valuable research information, but their value depend on the mathematical model used in the calculations. Therefore, it is important to validate them based on the physical modeling and the industrial measurements. The performed numerical and physical simulations and industrial measurements of the liquid steel flow in the one strand

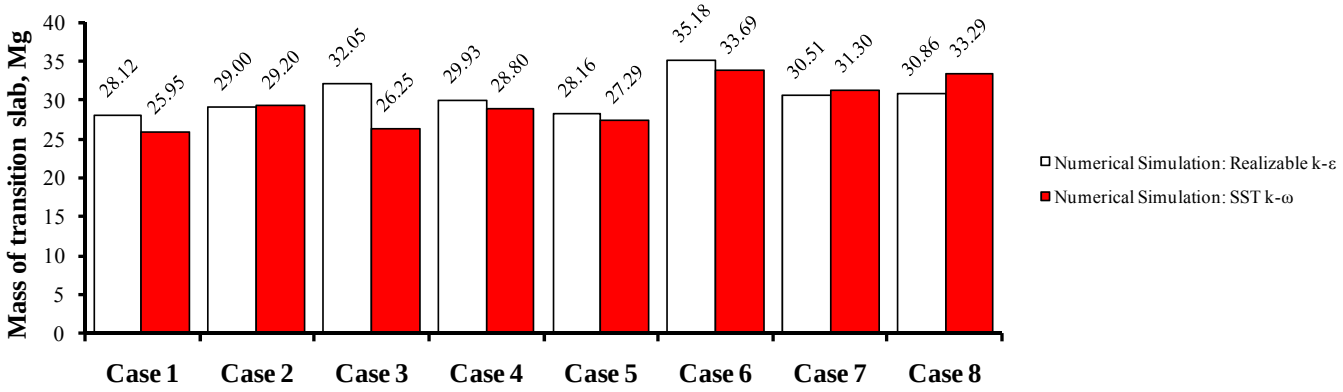

Fig. 8. The masses of the transition slab using the Realizable *k-ε* and SST *k-ω* turbulence models in the numerical simulations for the non-isothermal conditions

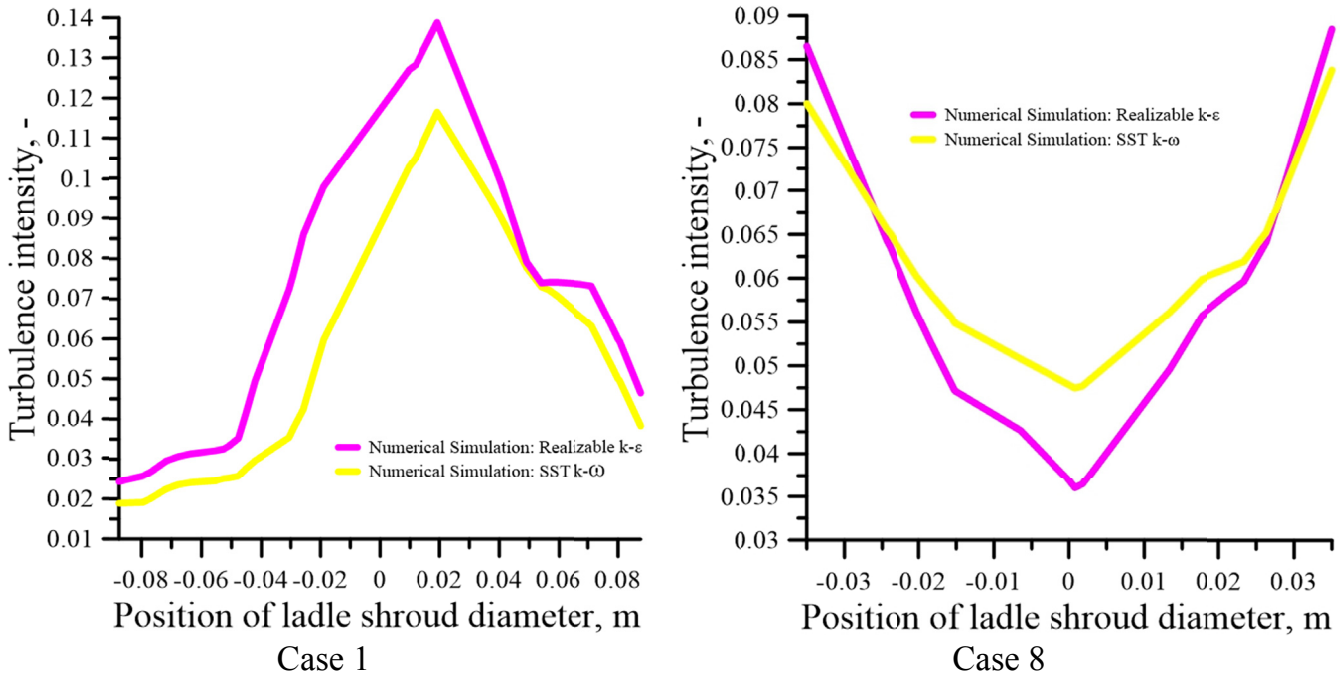

Fig. 9. The turbulence intensity recorded on the ladle shroud end using Realizable *k-ε* and SST *k-ω* turbulence models in the numerical simulations in the non-isothermal conditions

tundish confirm that the ladle shroud can be identified with FCD. Based on the research results, it was found that:

- The use in the numerical simulations the Realizable k-ε turbulence model caused the obtainment the outcomes similar to the results obtained from physical modeling (isothermal conditions).
- The results of the numerical calculations using the SST k-ω turbulence model correlates best with the outcomes from industrial measurements (non-isothermal conditions) among the tested turbulence models.
- The change of the MLS immersion depth in the liquid steel and STC installation influence on the hydrodynamic structure distribution in the tundish working space.
- The shortest range of the transition zone through immersing MLS on a depth of 0.1 m in the liquid steel for both turbulence models was achieved (the Realizable k-ε and SST k-ω).
- The use of MLS caused the lowering the turbulence intensity near the ladle shroud wall (at its end).

Acknowledgements

The research work carried out in the range of statutory research of the Department of Metallurgy and Metals Technology, Czestochowa University of Technology, no. of work BS/MN-204-301/2017.

The authors would like to thank the ISD Częstochowa Steelwork's CSC staff for their help in the industrial measurements.

REFERENCES

[1] M. Alizadeh, H. Edris, A.R. Pishevar, ISIJ Int. **48** (1), 28-37 (2008), DOI: doi.org/10.2355/isijinternational.48.28

[2] D. Mazumdar, R.I..L. Guthrie, ISIJ Int. **39** (6), 524-547 (1999), DOI: doi.org/10.2355/isijinternational.39.524

[3] A. Cwudziński, Steel Res. Int. **88** (9), 1600484 (2017), DOI: doi.org/10.1002/srin.201600484

[4] Y. Sahai, Metall. Mater. Trans. B **47** (4), 2095-2106 (2016), DOI: doi.org/10.1007/s11663-016-0648-3

[5] D. Chen, X. Xie, M. Long, M. Zhang, L. Zhang, Q. Liao, Metall. Mater. Trans. B **45** (2), 392-398 (2014), DOI: doi.org/10.1007/s11663-013-9941-6

[6] A. Espino-Zarate, R.D. Morales, A. Najra-Bastida, Metall. Mater. Trans. B **41** (5), 962-975, (2010), DOI: doi.org/10.1007/s11663-010-9398-9

[7] S. Joo, J.W. Han, R.I.L. Guthrie, Metall. Mater. Trans. B **24** (5), 767-777 (1993), DOI: doi.org/10.1007/BF02663137

[8] S. Joo, J.W. Han, R.I.L. Guthrie, Metall. Mater. Trans. B **24** (5), 779-788 (1993), DOI: doi.org/10.1007/BF02663138

[9] T. Merder, J. Pieprzyca, Steel Res. Int. **83** (11), 1029-1038 (2012), DOI: doi.org/10.1002/srin.201200059

[10] J. Zhang, S. Yang, J. Li, W. Yang, Y. Wang, X. Guo, ISIJ Int. **55** (8), 1684-1692 (2015), DOI: doi.org/10.2355/isijinternational.ISIJINT-2015-085

[11] G. Solorio-Diaz, R.D. Morales, J. Palafax-Ramos, L. Garcia-Demedices, A. Ramos-Banderas, ISIJ Int. **44** (6), 1024-1032 (2004), DOI: doi.org/10.2355/isijinternational.44.1024

[12] R.D. Morales, S. Garcia-Hernandez, J.D.J. Barreto, A. Ceballos-Huerta, I. Calderon-Ramos, E. Gutierrez, Metall. Mater. Trans. B, **47** (4), 2595-2606, (2016), DOI: doi.org/10.1007/s11663-016-0663-4

[13] J. Zhang, J. Li, Y. Yan, Z. Chen, S. Yang, J. Zhao, Z. Jiang, Metall. Mater. Trans. B, **47** (1), 495-507 (2016), DOI: doi.org/10.1007/s11663-015-0495-7

[14] A. Cwudziński, Metall. Res. Tech., **111**, (1), 45-55 (2014), DOI: doi.org/10.1051/metal/2014012

[15] A. Cwudziński, Steel Res. Int. **81** (2), 123-131 (2010), DOI: doi.org/10.1002/srin.200900060

[16] A. Cwudziński, Steel Res. Int. **85** (4), 623-631 (2014), DOI: doi.org/10.1002/srin.201300079

[17] A. Asad, Ch. Kratzsch, R. Schwarze, Steel Res. Int. **87** (2), 181-190 (2016), DOI: doi.org/10.1002/srin.201400600

[18] M.I.H. Siddiqui, P.K. Jha, ISIJ Int. **54** (11), 2578-2587 (2014), DOI: doi.org/10.2355/isijinternational.54.2578

[19] R.D. Morales, O. Davila-Maldonado, I. Calderon, K. Morales-Higa, ISIJ Int. **53** (5), 782-791 (2013), DOI: doi.org/10.2355/isijinternational.53.782

[20] M.J. Cho, I.C. Kim, ISIJ Int. **46** (10), 1416-1420 (2006), DOI: doi.org/10.2355/isijinternational.46.1416

[21] M.J. Cho, S.J. Kim, ISIJ Int. **50** (8), 1175-1179 (2010) DOI: doi.org/10.2355/isijinternational.50.1175

[22] Y. Sahai, T. Emi, ISIJ Int. **36** (9), 1166-1173 (1999), DOI: doi.org/10.2355/isijinternational.36.1166

[23] A. Vargas-Zamora, R.D. Morales, M. Diaz-Cruz, J. Palafox-Ramos, J.D.J. Barreto-Sandoval, Metall. Mater. Trans. B **35** (2), 247-257 (2004), DOI: doi.org/10.1007/s11663-004-0026-4

[24] S. Chakraborty, T. Hirose, J. Bill, D.A. Dukelow, Continuous Casting **10**, 41-46 (2003).

[25] B.G. Thomas, Continuous casting **10**, 115-127 (2003).

[26] A. Cwudziński, Ironmak. Steelmak. **37** (3), 169-180 (2010), DOI: doi.org/10.1179/030192309X12549935902383